Open Access Library Journal
2019, Volume 6, e5788
ISSN Online: 2333-9721
ISSN Print: 2333-9705

AVO Didactic Analysis from Simplified Modeling of Seismic Data in Libra Oil Field of the Pre-Salt Region, Brazil

Kaio da Silva Pimentel Figueiredo, Kaendra Williams Temoteo, Rafael Ximenes Gonçalves, Yasmim Monteiro Cordeiro, Rogério Manhães Soares, Hans Schmidt Santos, Claudiomar Rodrigues Franco, Felipe Barbosa Venâncio de Freitas, Christyne Barros de Sá

Faculdade Salesiana Maria Auxiliadora (FSMA), Macaé, Brazil

Email: hans.schmidt@live.com

How to cite this paper: Figueiredo, K. da S.P., Temoteo, K.W., Gonçalves, R.X., Cordeiro, Y.M., Soares, R.M., Santos, H.S., Franco, C.R., de Freitas, F.B.V. and de Sá, C.B. (2019) AVO Didactic Analysis from Simplified Modeling of Seismic Data in Libra Oil Field of the Pre-Salt Region, Brazil. *Open Access Library Journal*, **6**: e5788.
https://doi.org/10.4236/oalib.1105788

Received: September 16, 2019
Accepted: October 7, 2019
Published: October 10, 2019

Abstract

In this study, a certain zone of Libra oil field of the pre-salt region was selected to be analyzed for didactic purposes in order to simulate AVO responses. The region was modeled using seismic data, setting up a typical oil system with source rock (shale), reservoir rock (sandstone), and seal rock (salt). Thus, a set of parameters such as seismic wave velocity, density and Poisson's ratio for the studied zone was proposed. The AVO analysis allowed the classification of reflectors and the distinction of the geology for sandstones saturated with both water and gas.

Subject Areas

Environmental Sciences, Geology, Geomorphology, Geophysics

Keywords

Seismic, AVO, Pre-Salt, Libra Oil Field, Oil

1. Introduction

The main objective of the applied seismic is to obtain data with important information regarding the geology of the region where they were obtained. The seismic has many advantages, especially the ability to produce high definition images of the geological features. Furthermore, the seismic method may cover much larger areas compared to direct methods such as well drilling [1].

In seismic imaging, seismic waves are created through controlled sources and propagate across the subsurface. Some of these waves return after refraction and reflection on subsurface geological boundaries. Instruments distributed along the surface detect vibrations caused by these waves on their return and measure the arrival time at different distances from the source. These travel times are then converted into depths values, allowing subsurface geological interfaces to be systematically mapped [2].

The Libra oil field is one of the greatest discoveries in the Brazilian pre-salt. It is expected that in about 35 years this oil field will have produced 8 to 12 billion barrels of high-quality oil, API degree around 27 and very low sulfur content. The oil field is located 183 kilometers off the coast of Rio de Janeiro. It is in operation and has reached considerable depths exceeding the borders and the difficulties of the unknown [3].

The AVO analysis (amplitude versus offset) determines how changes in density, velocity, lithology, porosity, fluid contained, and thickness affect seismic response. It is used in data interpreting as a tool to reduce the risks involved in hydrocarbon exploration models [4].

The Brazilian pre-salt region stands out as the great discovery of recent years. In addition to the confirmed presence of large recoverable amounts, the pre-salt oil is considered of good quality and good price in the oil market [5]. In order to contribute to the research of such an important region for Brazil, AVO analysis was performed in a region representing a typical pre-salt oil system. Besides the scientific knowledge, this analysis may indicate the potential of the AVO method when applied in the pre-salt region.

Therefore, through variation of layers position, velocity of seismic waves, density and Poisson's ratio, the AVO analysis from seismic data in Libra oil field of the pre-salt region was carried out with the objective of simulating simplified geological models of seismic sections and performing the analysis of models through seismograms and classification of AVO anomalies (amplitude vs. offset).

Thus, Section 2 in this paper summarizes the theoretical basis of the reflection coefficients, synthetic seismograms and AVO analysis, which are necessary information to the understanding of the ensuing section. Section 3 identifies the data processing and demonstrates the results with figures and graphs. Section 4 summarizes the main results and conclusions.

2. Theoretical Foundations

2.1. Reflection Coefficient

According to Hafez (2017) [6], the earth subsurface comprises stratified rock layers that have different elastic properties. The boundaries separating the individual layers are referred as interfaces (**Figure 1**).

The wave transmission and reflection coefficients are obtained from the partition of amplitudes that occurs when an incident plane wave strikes a plane interface separating two elastic, homogeneous, isotropic, and semi-infinite layers [7].

According to Yenwongfai (2011) [4], an incident P-wave striking orthogonally the interface generates only other P-waves (reflected and transmitted). However, when the impact is not orthogonal, a pair of S waves (reflected and transmitted) is also generated as shown in **Figure 2**.

The waves at the interface are reflected and refracted according to Snell's Law (Equation (1)).

$$\frac{\sin\theta_1}{\sin\theta_2} = \frac{v_1}{v_2} \tag{1}$$

The reflection coefficient can be defined as Shuey approximation to Zoeppritz equations providing the angular dependence of the reflection coefficient $R_{(\theta)}$ of the P wave with two parameters: the intercept AVO (A) and the AVO gradient (B) (Equation (2)) [9].

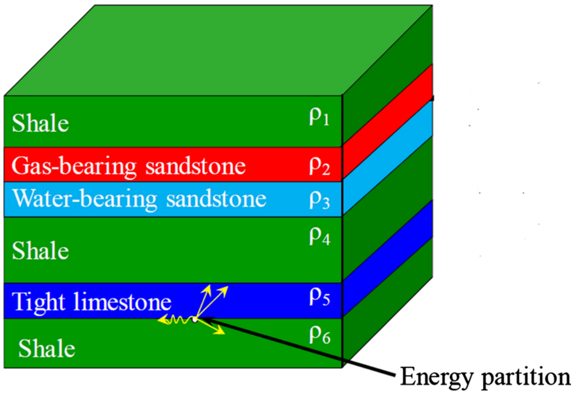

Figure 1. Energy partition on interfaces. Interfaces represent contact between two different pore fluids in same lithology or contact between two different lithologies [6].

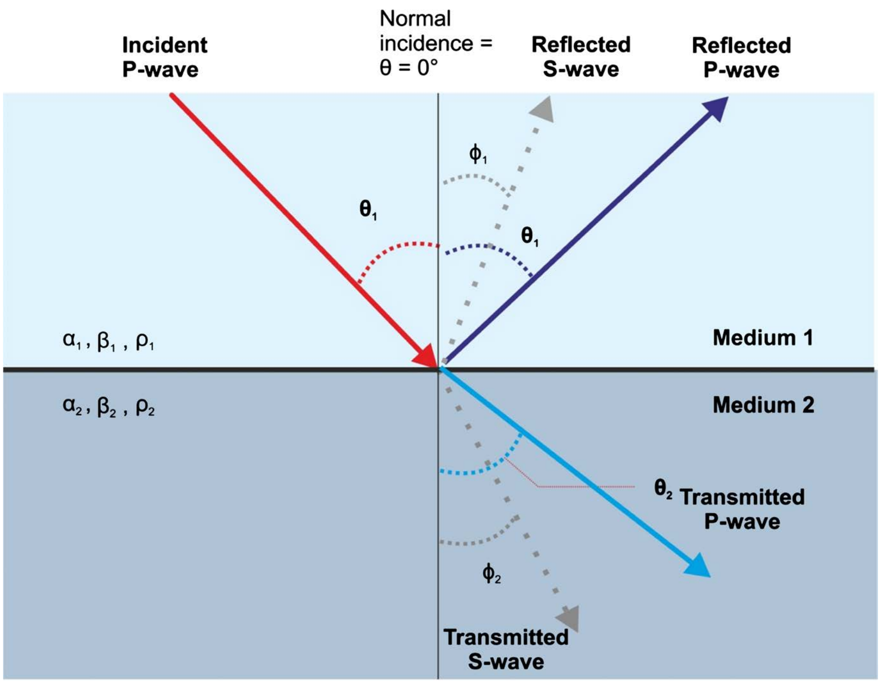

Figure 2. Transmission and reflection of P-waves in a plane interface showing the consequential transmitted and reflected P and S waves [8].

$$R_{(\theta)} = A + B\sin^2(\theta) \tag{2}$$

In practice, the "A" is a measure of the amplitude of normal incidence, indicating the normal reflection coefficient when $\theta = 90^\circ$ and "B" is a measure of amplitude variation with offset [9].

2.2. Synthetic Seismograms

From the view of seismic acquisition, seismic trace is a measure of time associated with a source-receptor pair. The distance between the source and the receptor is referred as offset. The main parameters used to generate a synthetic seismogram are density and speed that provide acoustic impedance, besides the waveform used, which is called wavelet [4].

The reflectivity relates layers with contrasting acoustic impedances. Thus, the reflection coefficients are calculated to determine the density and velocity profiles. However, the reflection coefficients are a function of depth, then a conversion to time is necessary. This conversion can be accomplished by choosing a sampling time, transforming speed profiles, which are a function of depth to profiles in transit time function [10].

Thus, the seismic traces are formed by a process called "convolution" of a series of reflection coefficients with a predefined wavelet (Equation (3)).

$$S_{(t)} = w_{(t)}r_{(t)} \tag{3}$$

In which $S_{(t)}$ is the synthetic seismic trace, $w_{(t)}$ is the wavelet and $r_{(t)}$ is the reflectivity. Figure 3 illustrates this process.

2.3. AVO Analysis

The AVO (Amplitude Versus Offset) analysis has been widely used in the oil and gas industry. This methodology is based on seismic amplitude response in a remote receptor. In addition to direct amplitude analysis, the graphs of the reflection coefficients from the top and the base of the reservoir allow the AVO classification

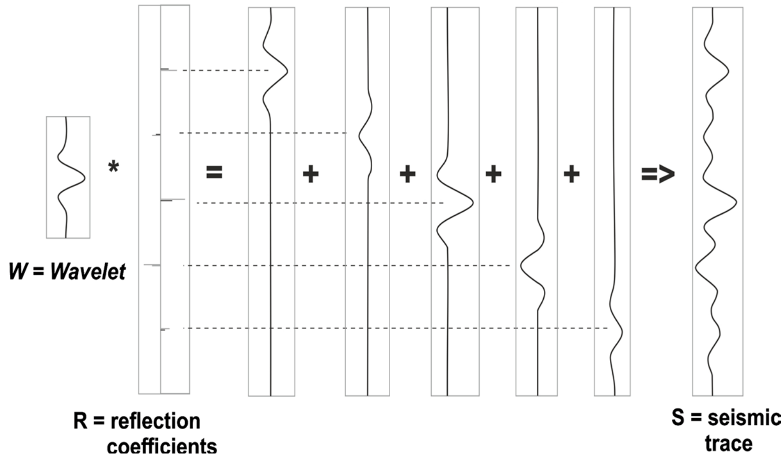

Figure 3. Convolutional model in the formation of seismic trace from reflection coefficients and wavelet [9].

associated to anomalies, which may be a support tool of hydrocarbon indication [10].

According to Ahmed *et al.* (2017) [11], the AVO analysis has been used in hydrocarbon exploration due to be able to discriminate the hydrocarbon fluids from background geology. Conventionally, AVO analysis involves calculation of intercept and gradient from a linear fit of compressional wave reflection coefficient to the sine square of the incidence angle as Equation (2).

The AVO study allows to predict the variation of the reflector amplitude as a function of the source-receiver distance. Often, with this study, it is possible to infer the type of fluid and its distribution in a certain rock, mostly considered to be isotropic [7].

The AVO modeling is an applied technique that allows the determination of the manner in which changes in density, velocity, lithology, porosity, fluid content, and thickness affect a seismic response [9].

According to Yenwongfai (2011) [4], the AVO anomalies are generally divided into four classes (**Figure 4**) depending on the coefficients of Equation (2).

Class I

The class I anomaly occurs when the normal incidence reflection coefficient (A) is strongly positive, showing a reduced amplitude with offset and the possible change in polarity for larger offsets, e.g. mature sands highly compressed in onshore environments.

Class II

The class II occurs when the normal incidence reflection coefficient (A) is small. Polarity changes may occur for near or moderate offsets. Some authors subdivide the anomaly into type II and IIp. In type II anomaly, the coefficient

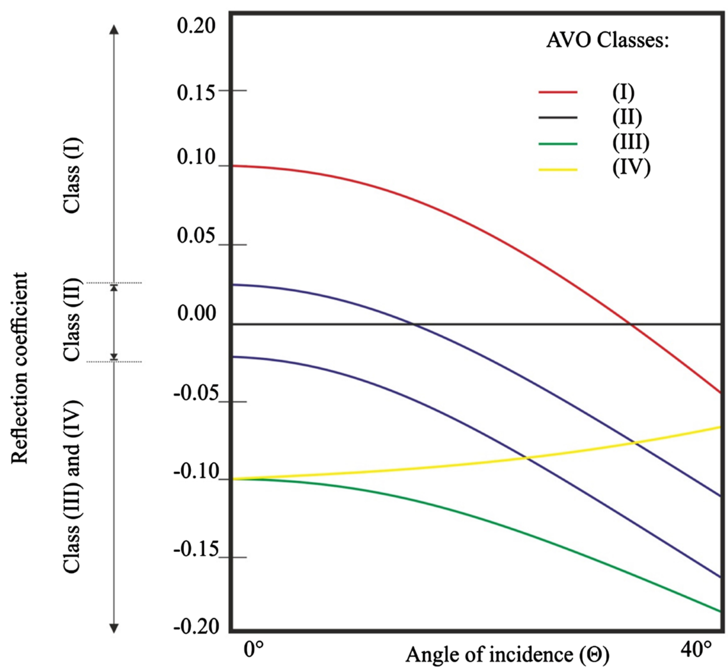

Figure 4. AVO classes for reflection coefficient versus offset [9].

(A) from Equation (2) is slightly positive, but with reverse polarity obtained because of displacement, it becomes slightly negative. In type IIp anomaly, coefficient (A) from Equation (2) is slightly negative, becoming more negative with the displacement e.g. sands showing median compression levels, common in offshore and onshore environments.

Class III

The class III anomaly occurs when the normal incidence reflection coefficient (A) is negative, becoming even more negative with the distance from source-receptor. In this case, there is a large reflectivity at all offsets, commonly being called bright spot anomaly occurring in typical marine sands.

Class IV

The Class IV anomaly is a subdivision of Class III. In this case, the coefficient at normal incidence (A) is negative, but the AVO gradient (B) has an anomalous behavior, being positive. This class is related to the presence of gas with inferior velocity compared to overlapping rock, thereby the amplitude decreases with the distance. Some sands of this class occur in the marine environment.

The classes of anomaly can be quickly interpreted through the crossploting graph (**Figure 5**) of the coefficients A and B from Equation (2).

The analysis of crossplot (A × B) is widely used to interpret AVO anomalies and infer the type of fluid in the pores of a rock. Since some rocks trend deviations can be hydrocarbon indicators [10].

The analysis of the anomalies and crossplot A × B was synthesized by Castagna and Swan (1997) [9] shown in **Table 1**.

3. Processing and Results

In data processing, 2D seismic sections from Libra oil field were used for the preparation of geological models through SeisMod 1.04 software from Protolink. In all processing, it was used Ricker wavelet centered on the frequency 33 Hz as shown in **Figure 6**.

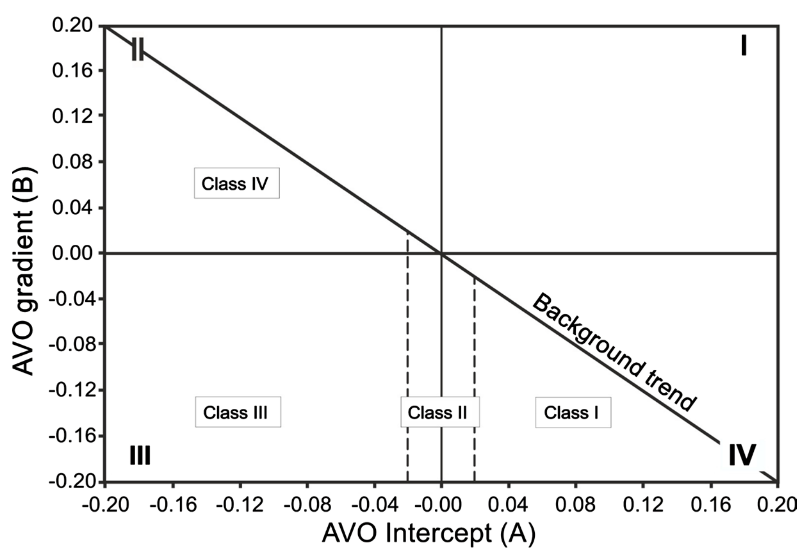

Figure 5. Classification based on the reflection position in crossplot (A × B) [9].

Table 1. AVO behavior for different impedance contrasts [9].

Class	Relative impedance	Quadrant	A	B	AVO
I	Greater than overlying unity	IV	+	−	decreases
II	Similar to the overlying unit	III or IV	±	−	increases or decreases
III	Less than overlying unity	III	−	+	increases
IV	Less than overlying unity	II	−	+	decreases

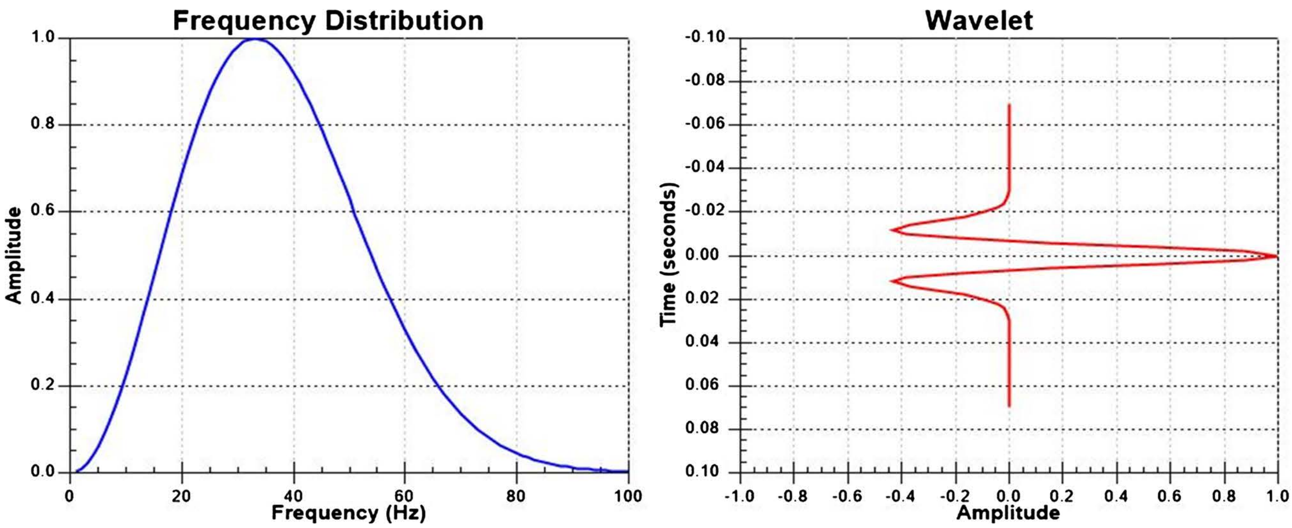

Figure 6. Ricker wavelet (called Mexican hat) centered at 33 Hz used in seismic trace formation.

We created models varying parameters such as layer positions, seismic wave velocity, densities, and Poisson's ratio. The reservoir rock considered was sandstone, on which two models were constructed: values for saturation with water and values for saturation with gas. These properties were used to describe the previously selected region through inputs in SeisMod 1.04 software as shown in Figure 7. Thus, allowing one to analyze the behavior of two different scenarios.

A reservoir region has been chosen to be tested. The tests were performed with rock saturated with water and then saturated with gas.

3.1. Simulating and Analysis of the Region

The study region has as interfaces the base of the salt and the base of the sag regions, being indicated by an arrow, according to Figure 8.

The simulated model is composed by three rock layers, chosen according to the geological model of the proposed region, configuring a possible "trap" with the source, reservoir and seal rocks of an oil system. Figure 9 highlights the region shown in Figure 8.

3.2. Test Area—Sandstone Saturated with Water and Gas

The region anomaly was verified by using values of sandstone filled with water and gas (Table 2).

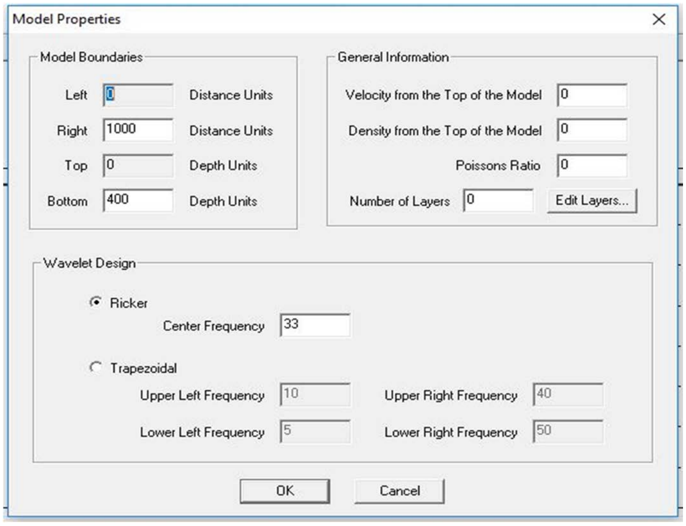

Figure 7. Model properties in SeisMod 1.04 software. In addition to the position and number of layers, it is possible to define three quantities: Poisson's ratio, density and velocity.

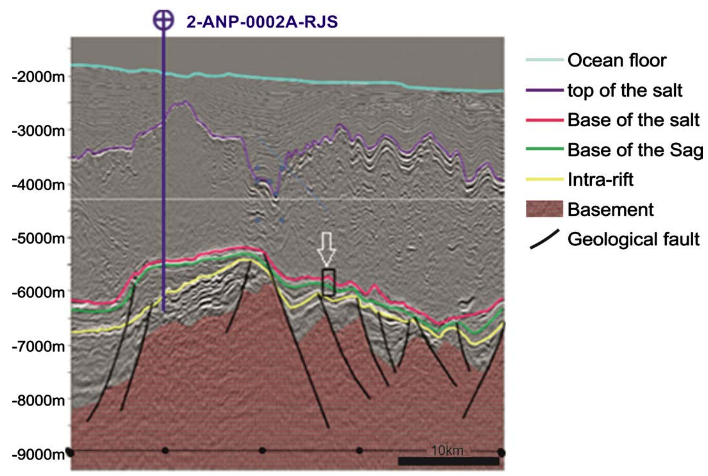

Figure 8. Study area of the Pre-Salt region. The white arrow indicates the region used in the simulations.

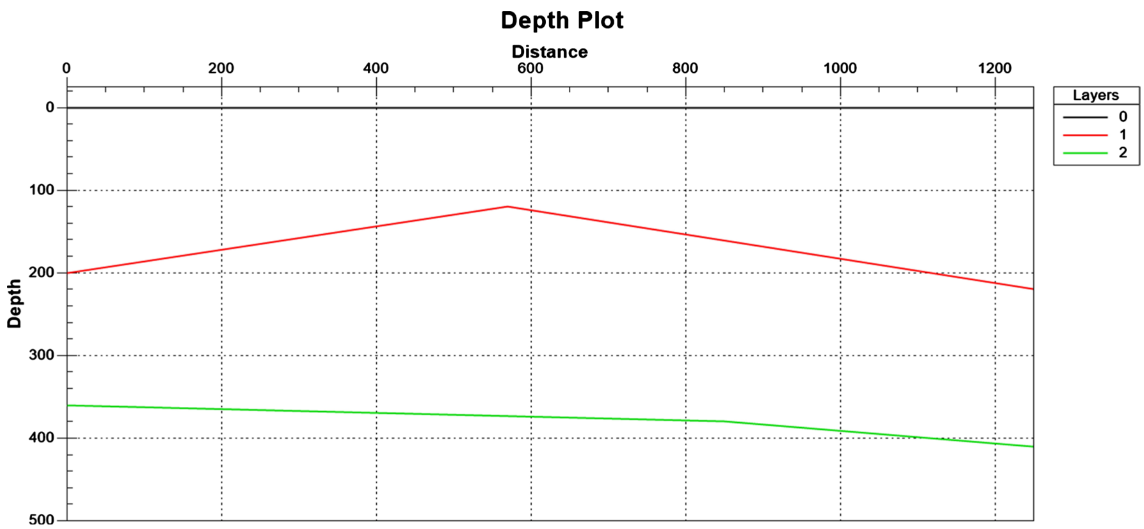

Figure 9. Geological model of the region with the salt base in red and the sag base in green.

Through SeisMod 1.04 software from Protolink, it was possible to obtain the seismogram of the region (Figure 10 and Figure 11), its reflection coefficient (Figure 12 and Figure 13), and the crossplot (Figure 14 and Figure 15), allowing us to classify the anomalies.

Table 2. Values of sandstone with water and gas.

Water Saturated Sandstone	Gas Saturated Sandstone
Caprock: layer 0—Gypsum (speed: 2750 m/s; density: 2.35 g/cm^3; Poisson constant: 0.22)	Caprock: layer 0—Gypsum (speed: 2750 m/s; density: 2.35 g/cm^3; Poisson constant: 0.22)
Reservoir rock: layer 1: Sandstone with water (speed: 3000 m/s; density: 2.25 g/cm^3; Poisson constant: 0.15)	Reservoir rock: Sandstone with gas (speed: 2700 m/s; density: 2.10 g/cm^3; Poisson constant: 0.15)
Source rock: Layer 2—shale (speed: 2500 m/s; density: 2.36 g/cm^3; Poisson constant: 0.355)	Source rock: Layer 2—shale (speed: 2500 m/s; density: 2.36 g/cm^3; Poisson constant: 0.355)

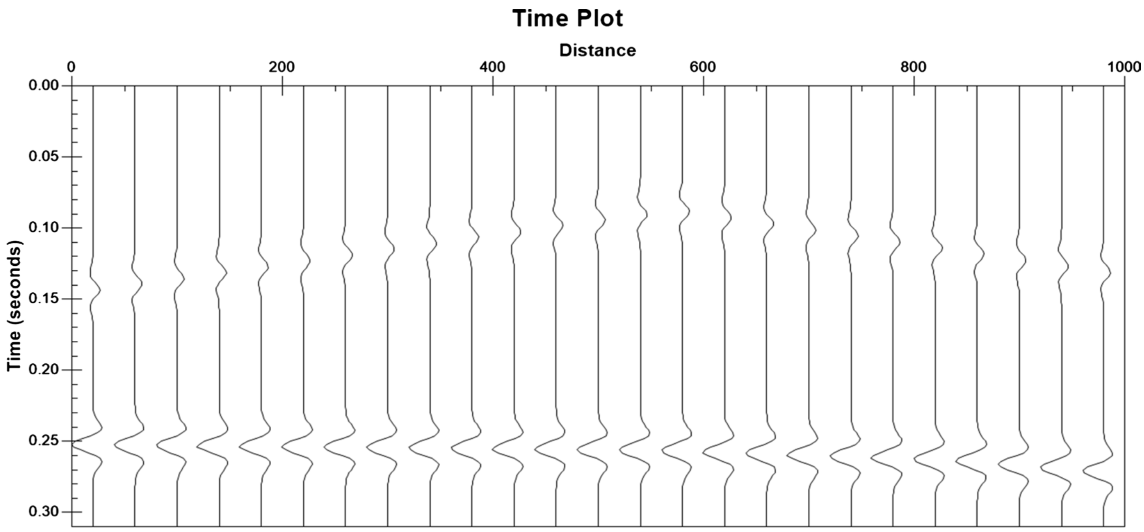

Figure 10. Seismogram of region (sandstone filled with water). The input reflector presented a positive amplitude anomaly.

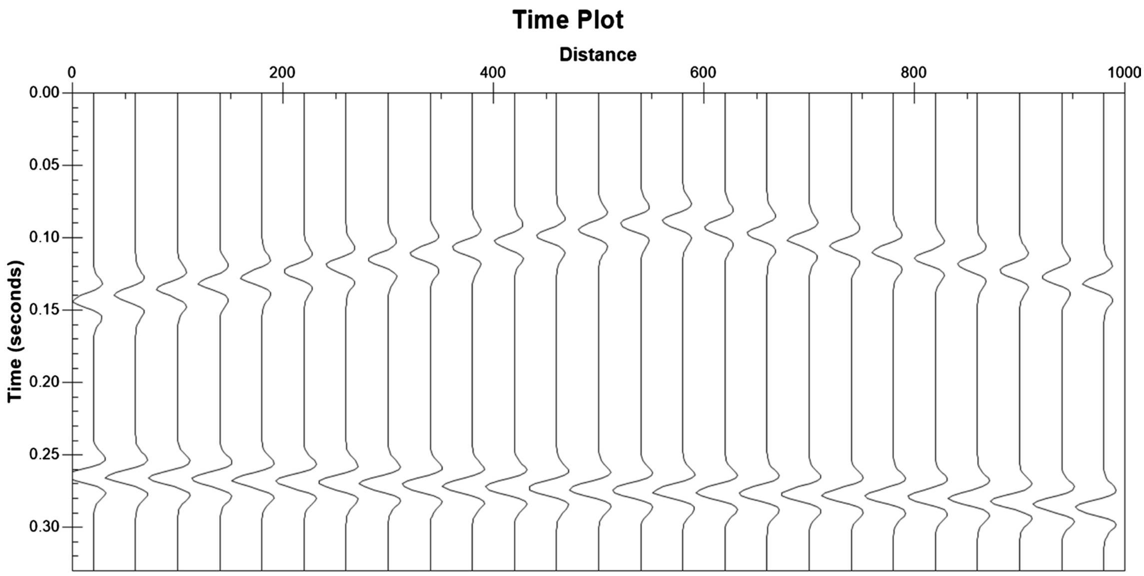

Figure 11. Seismogram of region (sandstone filled with gas). The input reflector presented a negative amplitude anomaly.

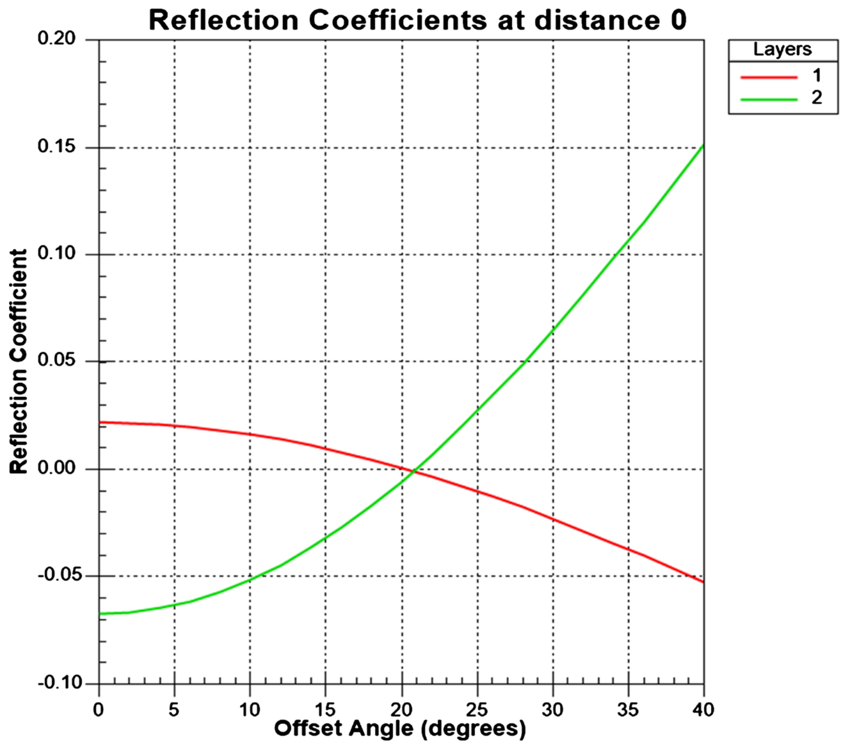

Figure 12. Reflection coefficient of the region based on sandstone with water. The reflection coefficient of the first layer starts positive, but it becomes negative with increasing offset.

Figure 13. Reflection coefficient of the region based on sandstone with gas. The reflection coefficient of the first layer starts negative and becomes more negative with increasing offset.

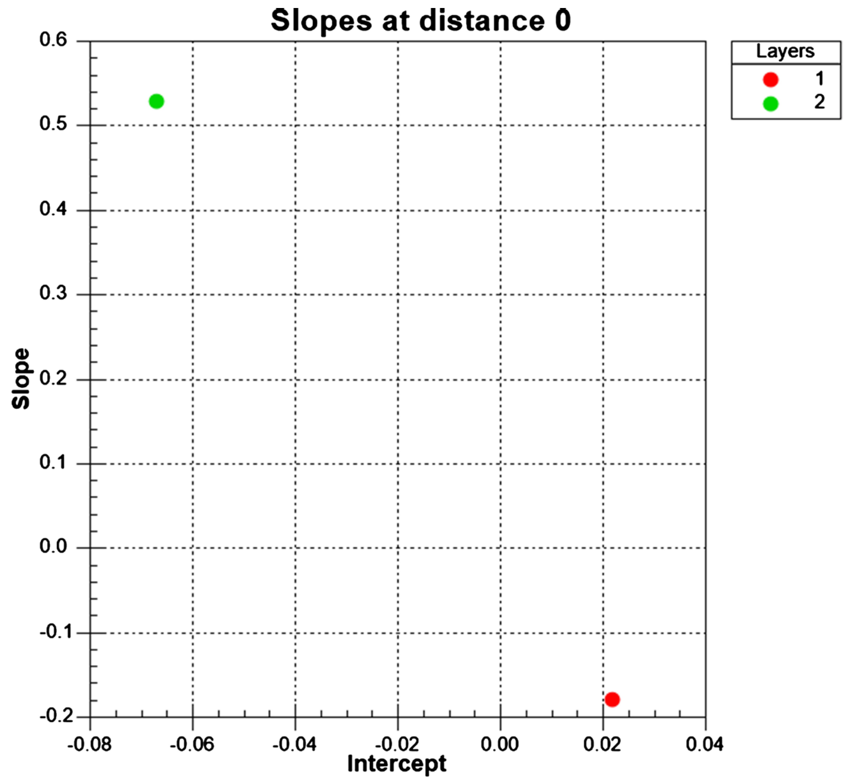

Figure 14. Crossplot of the region based on sandstone with water. The red dot shows that the reflection coefficient of the first layer is positive for 0 degree of offset.

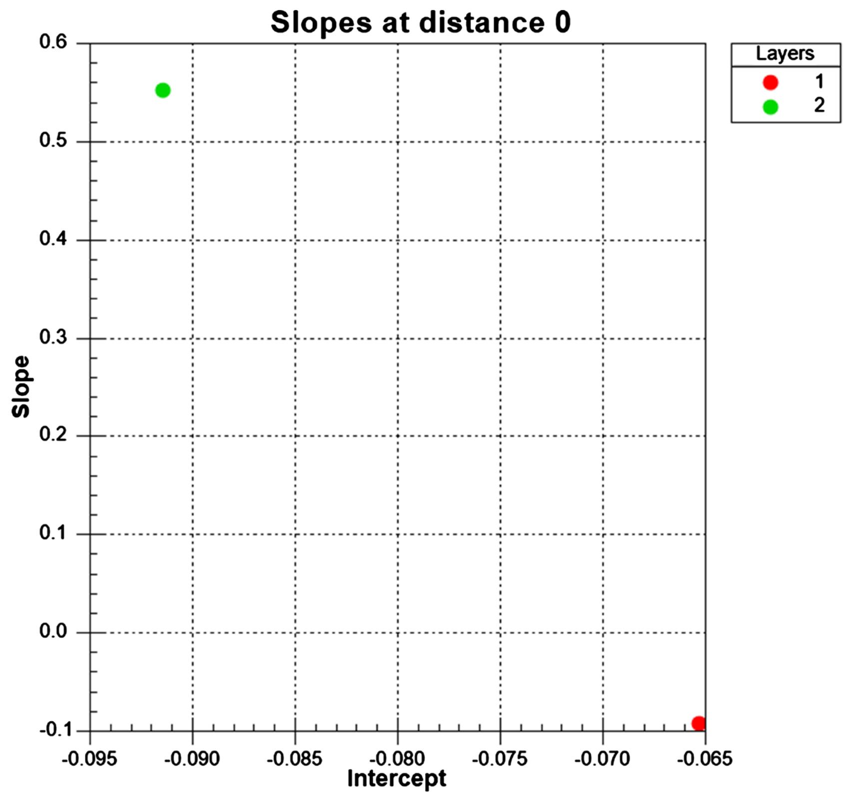

Figure 15. Crossplot of the region based on sandstone with gas. The red dot shows that the reflection coefficient of the first layer is negative for 0 degree of offset.

Seismogram analysis of sandstone filled with water (**Figure 10**) revealed that the input reflector presented a positive amplitude anomaly, meaning that the acoustic impedance of the sandstone layer filled with water is greater than the impedance anomaly of the overlying salt layer (gypsum). On the other hand, the anomaly of the output reflector is negative, denoting that the acoustic impedance of the shale layer is less than the acoustic impedance of the sandstone layer.

Seismogram analysis of sandstone filled with gas (**Figure 11**) revealed that the input reflector presented negative amplitude anomaly, meaning that the acoustic impedance of the sandstone filled with gas is smaller than the acoustic impedance of the overlying salt layer (gypsum). The output reflector anomaly remained negative, denoting that the acoustic impedance of the shale layer is lower than the acoustic impedance of the sandstone layer. Furthermore, it was noticed a slight delay in the response using the gas saturated system due to a lower wave velocity in sandstone saturated with gas.

The AVO analysis (**Figure 12**) denotes that layer 1 (red) has an anomaly classified as a Class II because the reflection coefficient of the first layer starts small and positive, but it becomes negative with increasing offset. According to the crossplot graph (**Figure 14**), the same anomaly can be observed. It is observed that layer 1 (red) is in the region of class II anomalies.

When the sandstone parameter is changed, now saturated with gas (**Figure 13**), we obtain a new type of anomaly in layer 1 (red), where analyzing the graph of the reflection coefficient and comparing with the characteristics of the anomalies, we conclude that layer 1 can now be classified as a Class III because the reflection coefficient of the first layer starts negative and becomes more negative with increasing offset. According to the new crossplot graph of the region (**Figure 15**), the same anomaly can be observed. It is observed that layer 1 (red) is in the region of class III anomalies. That is, lowering the acoustic impedance of the sandstone results in negative reflection coefficients, changing the anomaly from II to III with the change in saturation from water to gas.

4. Conclusions

In this work, a simplified geological model from Libra oil field of the pre-salt region was built in order to simulate AVO responses. The proposed geology was divided into seal rock, reservoir rock and source rock. Through variation of parameters such as P wave velocity, density and Poisson's ratio, seismograms responses were constructed.

Three types of geology were considered in the data processing and analysis from average values: salt layer, sandstone layer and shales. Moreover, parameter exchange procedures were performed in order to analyze didactically two different scenarios as reservoir rock saturated with water or gas. The analysis of seismograms helped to differentiate the gas saturated sandstone from water saturated sandstone through inversion of the positive amplitude anomaly to negative due to the reduction of acoustic impedance of the sandstone when filled with hydrocarbon.

This analysis, besides teaching, can point out the potentiality of the AVO method when applied in the Pre-Salt region by simulating the typical geology of the area in question.

The AVO anomaly analysis proved effectiveness in distinguishing petroleum systems with rocks saturated with water and rocks saturated with gas by changing anomaly from type II (positive reflection coefficients) to type III (negative reflection coefficients) in the input reflector. However, it should be noted that the AVO tool is only a support in the seismic interpretation, and it is not a direct indicator of hydrocarbons, since the parameters of the rocks (velocity, density and Poisson ratio) can vary widely for different reasons.

For future work, the use of different rocks and configurations is recommended, so the anomalies that did not occur in the examples could be studied. In addition, it is recommended to study another region, so different rock parameters could be simulated.

Conflicts of Interest

The authors declare no conflicts of interest regarding the publication of this paper.

References

[1] Figueiredo, A.M. (2007) Mapeamento Automático de Horizontes e Falhas em Dados Sísmicos 3D baseado no algoritmo de Gás Neural Evolutivo. Master's Thesis, Pontifical Catholic University of Rio de Janeiro, Rio de Janeiro.

[2] Kearey, P., Brooks, M. and Hill, I. (2002) An Introduction to Geophysical Exploration. Blackwell Science Ltd., Oxford.

[3] Ministério de Minas e Energia (2013) Nota sobre o Pré-sal e o campo de Libra. Portal Brazil.

[4] Yenwongfai, H.D. (2011) Compaction, Rock Properties and Avo Modeling in the Goliat Field, SW Barents Sea. Master's Thesis, University of Oslo, Oslo.

[5] Gouveia, F. (2010) Tecnologia nacional para extrair petróleo e gás do pré-sal. *Conhecimento e Inovação*, **6**, 30-35.

[6] Hafez, A. (2017) Seismic Attributes and AVO Analysis. Cairo Egypt.

[7] Nascimento, F. (2010) Estudo das Classes de Anomalias de AVO. Thesis, UFF, Niteroi.

[8] Almutlaq, M.H. and Margrave, G.F. (2010) AVO Inversion. CREWES Research Report, Vol. 22, 1-23.

[9] Castagna, J.P. and Swan, H.W. (1997) Principles of AVO Cross Plotting. *The Leading Edge*, **6**, 337-344. https://doi.org/10.1190/1.1437626

[10] Piauilino, L.S. (2014) Análise de AVO para caracterização de um reservatório clástico na Bacia Sedimentar do Oeste do Canadá. UFF, Niteroi.

[11] Ahmed, N., Khalid, P., Ghazi, S. and Anwar, A.W. (2015) AVO forward Modeling and Attributes Analysis for Fluid's Identification: A Case Study. *Acta Geodaetica et Geophysica*, **50**, 377-390. https://doi.org/10.1007/s40328-014-0097-x